A closed-loop brain-machine interface to modulate pain

Qiaosheng Zhang[1], Sile Hu[2], Robert Talay[1], Amrita Singh[1], Bassir Caravan[2], Zhengdong Xiao[2], David Rosenberg[2], Anna Li[1], Johnathan D. Gould[3], Zhe S. Chen[2,4,5*] & Jing Wang[1,4,5*]

1. Department of Anesthesiology, Perioperative Care and Pain, New York University School of Medicine, New York, NY 10016

2. Department of Psychiatry, New York University School of Medicine, New York, NY 10016

3. College of Arts and Sciences, New York University, New York, NY 10003

4. Department of Neuroscience & Physiology, New York University School of Medicine, New York, NY 10016

5. Neuroscience Institute, NYU Langone Health, New York, NY 10016

Correspondence: *Equal contribution. zhe.chen@nyulangone.org (ZSC) and jing.wang2@nyulangone.org (JW)

A key challenge for the study and treatment of neuropsychiatric diseases is to target pathological neural activities with high temporal resolution. Pain is a fundamental sensory-affective experience, and chronic pain, a disorder that affects one in three adults, comprises discrete symptomatic episodes of unpredictable timing and frequency[1]. Non-adaptive, continuous treatments for pain, especially chronic pain, are associated with poor efficacy and untoward side effects including addiction. Brain-machine interface (BMI) offers a potential solution to this challenge. BMIs have been developed to detect and ablate epileptic events and to link cortical commands with prosthetic devices for motor control[2-15]. Here we

have engineered a BMI to uniquely modulate the sensory-affective experience in rats by coupling neural codes for nociception directly with therapeutic cortical stimulation in a closed-loop system. We record neural activities in the anterior cingulate cortex (ACC), a region that is critical for pain processing[16-23], in freely behaving rats, and decode the onset of evoked pain episodes in real time based on ensembles of online sorted spikes[24,25]. We then couple this pain onset detection with optogenetic activation of the prelimbic prefrontal cortex (PFC), a region well-known to provide descending pain inhibition in rodents[26-30]. Our closed-loop BMI not only effectively inhibits sensory and affective components of acute mechanical and thermal pain, but also detects and relieves sensory hypersensitivity and enhanced aversion associated with chronic pain. Furthermore, this system enables the identification and regulation of tonic pain. Together, these findings support the closed-loop neuromodulation strategy for both pain therapy and the study of pain mechanisms. More generally, these results provide a blueprint for the development of BMIs to target neuropsychiatric disorders affecting the sensory and affective systems.

To design a closed-loop BMI for pain, we paired a detection arm with a treatment arm (Fig. 1a). For pain detection, we recorded neural activity from the ACC with silicon probes (Fig. 1b and Extended Data Fig. 1). Numerous studies have shown that the ACC is critical for pain processing[16-23]. Recently, we and others have demonstrated that neural signals from the ACC, including spike activities, can be used to decode the intensity and timing of pain with good sensitivity and specificity[24,25,31]. We have developed a state-space model (SSM) to detect the onset of pain experience based upon ensemble spike activity in the ACC (Methods; Fig. 1c, and Extended Data Fig. 2a). With this SSM-based strategy, we identify a proxy for the acute pain

signal that drives the observed population spike activity, thus formulating pain onset detection as detection of a change from the putative baseline condition. This model-based strategy has revealed that the latent processes driving ACC neuronal activities correlate to the onset of observed pain behavior with high degrees of accuracy and temporal precision[24,25]. Furthermore, the performance of our strategy for detecting pain onset is robust with both well-isolated offline sorted single units and multi-unit activity, thus facilitating its application with online sorted spikes[24]. For the treatment arm, we used optogenetic activation of the prelimbic region of the PFC (Extended Data Fig. 1b), as previous work has shown that the activation of this region provides effective relief of sensory and affective pain symptoms via descending projections in rodents[26-30]. To assist online model parameter selection and data visualization, we designed a custom graphic user interface (GUI) to integrate the pain detection arm with the treatment arm (Extended Data Fig. 2b), forming a closed-loop neural interface.

We first applied this real-time BMI in the context of acute thermal pain. We used a calibrated infrared (IR) generator from the Hargreaves' pain assessment toolkit to deliver a noxious stimulus at high IR intensity, and a non-noxious stimulus at low IR intensity to the hind paws of rats (Fig. 2a, b). As shown previously, ACC neurons contralateral to the site of peripheral stimulation increased their firing rates in response to the noxious thermal stimulus (Extended Data Fig. 3)[31]. In contrast, the non-noxious stimulus did not produce significantly increased spiking activities in the same neurons (Extended Data Fig. 3). We then applied our SSM-based decoding strategy to detect the onset of pain experience in real time by identifying a change in online sorted ACC ensemble spikes (Extended Data Fig. 2). Our model-based strategy detected pain onset reliably after the presentation of noxious stimulus, with high temporal precision (Fig.

2c). The SSM-based decoder was able to detect up to 75% evoked thermal pain episodes, with few false detections (Fig. 2d, e and Extended Data Table 1). In a majority of the cases, detection occurred after the presentation of noxious stimulus but prior to paw withdrawals, suggesting that cortical nociceptive response precedes behavioral response (Fig. 2f, g). This temporal delay also indicates the possibility for a closed-loop system to intervene in pain behaviors in real time immediately after pain detection. Thus, we coupled pain onset detection with optogenetic activation of the prelimbic PFC contralateral to the ACC recording sites (Fig. 1 and Extended Data Fig. 1). PFC activation triggered by the SSM in our closed-loop BMI prolonged paw withdrawal latency on the Hargreaves' test (Fig. 2f, h), demonstrating pain relief. This pain-inhibitory effect provided by the BMI was as strong as constitutive, manually controlled prelimbic PFC activation, further validating the capability of this closed-loop neuromodulation system to inhibit acute thermal pain. Next, we used pin prick (PP) to deliver mechanical pain to the hind paws of rats (Fig. 2i, j). In contrast to IR, PP caused almost instantaneous withdrawal response. Nevertheless, ACC neurons increased their firing rates in response to noxious stimulations, in contrast to non-noxious stimulations (von Frey filaments, or vF) (Extended Data Fig. 4). Our SSM-based decoder accurately detected ~60% of evoked mechanical pain episodes (Fig. 2k-m, and Extended Data Table 1). We then used a classic conditioned place aversion (CPA) assay to assess the ability of the BMI to control the aversive response to mechanical pain[31-34]. During the conditioning phase, we applied noxious stimulations (PP) to the rats' hind paws in both treatment chambers (Fig. 2n). In one of these chambers, rats received automated, BMI-triggered therapeutic PFC activation. In the opposite chamber, rats received randomly delivered PFC stimulations of matching duration and intensity. After conditioning, rats preferred the chamber associated with the BMI treatment (Fig. 2o-q). In contrast, rats did not develop such

preference for the BMI treatment when the peripheral stimuli were non-noxious, indicating that PFC stimulation delivered by the BMI was not intrinsically rewarding or aversive (Extended Data Fig. 5). These results demonstrate that a closed-loop system coupling therapeutic PFC activation with decoded pain episodes based on ACC activities inhibits both sensory and affective behavioral response to acute pain. At the cellular level, activation by BMI reduced the peak and cumulative firing rates of ACC pyramidal neurons after noxious stimulations (Fig. 2r-t). This temporally specific link between reduced ACC neuronal activity and decreased pain aversion validates a causal effect between ACC activity and affective pain behaviors that has been suggested in previous studies[20,31]. Therefore, a closed-loop BMI can not only deliver therapeutic interventions in real time, but also enable studies of causal inference for the neural basis of pain.

Next, we investigated whether this closed-loop BMI could be used to inhibit behaviors associated with chronic pain. Two hallmark features of chronic pain are hypersensitivity to peripheral stimuli and tonic or spontaneous pain. We first assessed hypersensitivity in a well-established inflammatory pain model (Complete Freund's Adjuvant or CFA model, Fig. 3a). As expected[31], CFA-treated rats developed sensory allodynia to mechanical von Frey filament (vF) stimulations, as manifested by paw withdrawal responses (Fig. 3b and Extended Data Fig. 6). Our neural decoding analysis was able to distinguish a 6g vF stimulus sufficient to elicit nocifensive withdrawals from a 0.4g vF stimulus that did not consistently elicit withdrawals (Fig. 3c-e and Extended Data Table 1). These results indicate that our SSM-based decoder can detect allodynia events in real time as well as events triggered by noxious stimuli such as PP. BMI-driven activation of the prelimbic PFC, meanwhile, reduced mechanical allodynia (Fig. 3f). In

addition to peripheral hypersensitivity at the site of injury, chronic pain also causes an increased aversive response, which can be assessed by the conditioned place aversion (CPA) assay[27,31-34]. In one chamber, we paired a peripheral 6g vF stimulus (which is sufficient to induce allodynia) with BMI-driven activation of the PFC, and in the opposite chamber paired this stimulus with randomly delivered PFC activation (Fig. 3g). After conditioning, rats preferred the BMI-paired chamber (Fig. 3h-j). In contrast, rats did not prefer the BMI-paired chamber when they received a non-noxious, 0.4g vF stimulus during conditioning (Extended Data Fig. 7). We then repeated these experiments in a model of chronic neuropathic pain (Spared Nerve Injury or SNI)[26,35] (Fig. 3k, l and Extended Data Fig. 8). Again, our SSM could detect when rats received a 6g vF stimulus that elicited nocifensive withdrawals, versus when rats received a 0.4g vF stimulus that did not consistently elicit withdrawals (Fig. 3m-o and Extended Data Table 1). The BMI in turn reduced mechanical allodynia in the SNI model (Fig. 3p). In the CPA assay, we paired the 6g vF stimulus with either BMI-triggered or random PFC activation (Fig. 3q), and SNI-treated rats preferred the BMI-paired chamber (Fig. 3r-t). In contrast, rats showed no preference for the BMI-paired chamber if the peripheral stimulus was non-noxious (Extended Data Fig. 9). Together, these results demonstrate that peripheral allodynia in the chronic pain state produces similar neural responses in the ACC as acute noxious stimulations in naïve animals, and these neural responses can in turn be used to trigger closed-loop neurostimulation to inhibit sensory hypersensitivity and decrease aversion.

In addition to hypersensitivity to evoked stimuli, chronic pain also causes tonic or spontaneous pain[34]. Recent studies have shown that pharmacological or optogenetic interventions during the CPA assay can unmask the presence of tonic pain[26,34,36,37]. However, identifying the dynamic

neural processes that underlie individual spontaneous pain episodes remains an unmet challenge in both animal models and human subjects. The specificity and high temporal precision of the closed-loop BMI provides a potential solution to this problem. In CFA-treated rats, we paired one CPA chamber with BMI, and the other chamber with random activation of the PFC of matching duration and intensity, in the absence of additional peripheral stimulations (Fig. 4a). We hypothesized that the same decoding strategy we employed for evoked pain should detect individual spontaneous pain episodes to trigger PFC activation to relieve pain during a prolonged conditioning phase[38]. Remarkably, after training with an evoked stimulus, our decoder identified putative spontaneous pain events in the CFA model based on ACC ensemble spikes (Fig. 4b). The neural signature for these putative spontaneous pain events bears resemblance to the neural signature for evoked pain episodes (Fig. 3c). Importantly, after conditioning, rats developed preference for the chamber associated with BMI activation (Fig. 4c-e). Next, we tested the ability of the BMI for targeting tonic neuropathic pain in the SNI model (Fig. 4f). Our method provided similar tonic pain detection in the SNI model (Fig. 4g), and rats showed the same preference for the BMI treatment, suggesting that our closed-loop BMI could inhibit tonic pain (Fig. 4h-j). As PFC activation triggered by detected pain onset induces pain relief compared with random activation, the detected episodes have a high likelihood of being true spontaneous pain events. Therefore, our BMI can be a valuable tool for identifying spontaneous pain for mechanistic inquiries, similar to the application of the BMI technology in studies of motor learning[2]. To validate the capability of our closed-loop BMI to relieve tonic pain, we examined its efficacy at inhibiting paw-licking behaviors. Paw licking has been identified as a spontaneous pain behavior in inflammatory pain models[39-42]. Here we compared the number and total duration of paw licking episodes during a 10-min session, and found that the closed-loop BMI was effective in

reducing the paw-licking frequency and duration in the CFA model (Extended Data Fig. 10). These results further support the efficacy of the closed-loop BMI to detect and treat tonic pain in rodent models.

To date, treatment options for severe acute or chronic pain remain limited, and continuous pharmacological and neuromodulation therapies are associated with multiple side effects. Here we have engineered a closed-loop rodent BMI as a prototype demand-based neuromodulation system to inhibit symptoms of acute and chronic pain and to provide causal inference for mechanisms of nociception. Future refinement of this technology and its adaptation to humans hold promise for non-pharmacological treatment for pain. More generally, these results suggest the feasibility of closed-loop BMI to target sensory and affective processes associated with neuropsychiatric diseases.

METHODS

Experimental protocol, data acquisition and BMI system architecture

All experimental studies were performed in accordance with the New York University School of Medicine (NYUSOM) Institutional Animal Care and Use Committee and the National Institutes of Health (NIH) *Guide for the Care and Use of Laboratory Animals* to ensure minimal animal use and discomfort.

Virus construction and packaging

Recombinant AAV vectors were serotyped with AAV1 coat proteins and packaged at the UPenn vector core. Viral titers were 5×10^{12} particles per mL for AAV1.CaMKII.ChR2-eYFP.WPRE.hGH, and AAV1. CaMKII(1.3).eYFP.WPRE.hGH.

Viral injection

Rats were anesthetized with isoflurane (1.5 to 2%). In all experiments, virus was delivered to the prelimbic PFC only. Rats were unilaterally injected with 0.5 μL of viral vectors at a rate of 0.1 μL every 20 s with a 26-gauge 1 μL Hamilton syringe at anteroposterior (AP) +2.9 mm, mediolateral (ML) ±1.6 mm, and dorsoventral (DV) −3.7 mm, with tips angled 17° toward the midline. The microinjection needles were left in place for an additional 10 min, raised 1 mm, and left for another minute to allow for diffusion of virus particles away from injection site and to minimize spread of viral particles along the injection tract. After viral injections, the scalp was sutured and given three weeks for viral expression before optic fiber and electrode implantation.

Prelimbic PFC optic fiber and ACC silicon probe implantation surgery

Optic fiber and electrode implants were performed as described in previous studies[31,33]. We constructed custom fiber optic cannulae with 200 μm optic fibers held in 2.5 mm ferrules (Thorlabs) for prelimbic PFC optogenetic stimulation. 32-channel silicon probes (Buzsaki32-H32, NeuroNexus Technologies, or ASSY-116 E-1, Cambridge NeuroTech) were glued with 3D printed custom design drives or commercial dDrives (NeuroNexus) for ACC recording. During the implant, rats were anesthetized with isoflurane (1.5 to 2%). Optic fibers were implanted 0.5 mm right above prelimbic PFC viral injection spot (AP +2.9 mm, ML ±1.6 mm, DV -3.2 mm), with tips angled 17° toward the midline. Contralateral to the optical fiber implant, silicon probes

were implanted in the ACC (AP +2.7mm, ML±1.6 mm, DV -2.0 mm) with tips angled 22° toward the midline. Silicone artificial dura gel (Cambridge NeuroTech) was added to protect the dura. Vaseline was used for wrapping electrode movable parts, which include silicon probe shanks and flexible cables, and drive shuttle. Both optical fiber and drive were secured to the skull screws with dental cement. After surgery, rats were given one week to recover before neural recordings.

***In vivo* electrophysiological recordings and optogentic stimulation**

The hardware of the BMI system for pain experiments consists of following components: electrode arrays (with drives) and headstages, commutator, data acquisition system, Optic fiber cannulas, blue LED or blue laser, desktop computer, video cameras and other optional devices, as shown in Fig. 1 and Extended Data Fig. 1.

Animals with chronic optical fiber and electrode implants were given a 30 min period to habituate to a recording chamber over a mesh or glass table before recording. Silicon probes were connected with 32-ch digital headstages (HST/32D, Plexon) and wired through a motorized commutator (OPT/Carousel M Commutator 2LED-4DHST-TH, Plexon). Optic fiber cannulas were connected with a 465nm blue LED (OPT/LED_Blue_Compact_LC_magnetic, Plexon) through mating sleeves (ADAF2, Thorlabs) and fiber patch cables. The blue LED was magnetically mounted on the same carousel commutator.

Neural signals were recorded at 40 kHz through a 64-ch OmniPlex data acquisition system (Plexon). The spikes were thresholded from high-pass filtered (>300 Hz) raw neural signals and

further online spike sorted through 2D Polygon method (PlexonControl, Plexon). Only spikes with high signal-to-noise ratio (SNR>3) were selected for BMI population decoding. Online sorted spike time events were packaged and sent to BMI client software through Plexon application program interfaces with 50-ms bin size. The state space model would calculate the output inference of current latent variable based on the binned spike counts. The model would trigger an optogenetic stimulation if the threshold criteria was met. In the meantime, the raw neural signals, online sorted spikes, multiple event time stamps which included pain stimulus events, pain onset detection events, optogenetic stimulus events were recorded through PlexControl (Plexon) for further offline data analysis.

For optogenetic stimulation, the blue LED was controlled by OmniPlex digital 5V TTL output. And the optic fiber tip output power was calibrated before experiments. The parameters for optogenetic stimulation were 20 Hz with 10-ms pulse width, of 5-s duration.

During recording, three video cameras (DMK23U, Imaging Source, FDR-AX53, Sony) were used to record rat behavior and BMI client software online-decoding results. The cameras were synchronized with neural recording at the beginning of each recording session. Long inter-trial intervals between trials were used to avoid behavioral or neural sensitization.

State-space method for detecting the pain onset

Pain perception is a dynamic process, and the pain percept can be modeled as an abstract latent variable. In our previous work, we have formulated the problem of detecting the onset of pain signals as a change-point detection problem[24,25]. The detection problem was resolved by a state-

space method, where the state-space model (SSM) consists of a state equation and a measurement equation[43]. In the state equation, we assumed that the temporal neural activity $\boldsymbol{y}_k$ (k=1,…,K), represented by a C-dimensional vector, was driven by a common one-dimensional latent Markovian process z_k:

$$z_k = az_{k-1} + \epsilon_k$$

where ϵ_k specifies a temporal Gaussian prior (with zero mean and variance σ^2) on the latent process, and $0<|a|<1$ is the first-order autoregressive (AR) coefficient. In the measurement equation, we assumed the Poisson linear dynamical system (PLDS) for neuronal ensemble spikes, with the observation vector $\boldsymbol{y}_k$ consisting of spike count of C neurons (bin size Δ), where the logarithm of the neuronal firing rate, $\boldsymbol{\eta}_k$, is modulated by a weight factor in vector $\boldsymbol{c}$ plus a DC term $\boldsymbol{d}$

$$\boldsymbol{\eta}_k = \boldsymbol{c}z_k + \boldsymbol{d},$$

$$\boldsymbol{y}_k \sim Poisson(\exp(\boldsymbol{\eta}_k)\Delta),$$

The second equation is a generalized linear model (GLM) that employs an exponential link function through $\boldsymbol{\eta}_k$, where $\boldsymbol{y}_k$ is Poisson distributed with the rate parameter $\exp(\boldsymbol{\eta}_k)$.

Let Θ denote all unknown model parameters, and we have developed an iterative expectation-maximization (EM) algorithm to infer latent state sequences (E-step) and unknown parameters $\Theta=\{a, \boldsymbol{c}, \boldsymbol{d}, \sigma^2\}$ (M-step). Upon model identification, an online recursive filter was run to estimate the latent state estimate $\hat{z}_k$[24,25]. We then computed the Z-score related to the baseline: $\text{Z\_score} = \frac{z-\text{mean}(z_{\text{baseline}})}{\text{SD}(z_{\text{baseline}})}$ and further converted it to probability or one-tailed P-value[23]. We monitored the probability to assess the significance of change point detection. The criterion of Z-score change was determined by a critical threshold for reaching statistical significance. The first

time point that crossed the significance threshold for the change point was treated as the onset of pain. Using 95% significance level, it was concluded that when Z-score−CI > 1.65 or Z-score + CI < −1.65, where the CI denotes the confidence interval derived from the state posterior variance.

BMI software development

The BMI software that manages the operation of the system was run on a desktop PC (Intel Xeon E5-1620 CPU, 3.5 GHz, 48 GB memory, Window OS). The software supported the hardware platform for online neural decoding analysis and the graphic user interface (GUI).

The components and tasks of the BMI system was managed by a client software including the following modules: (i) data acquisition and buffering, (ii) online neural encoding/decoding algorithms, (iii) external device control, (iv) configuration management, and (v) user interfaces. We developed the software in C/C++ programming language along with the software developing toolkit provided by Plexon and other open-source software packages. To accommodate maximum flexibility while minimizing the complexity of maintenance, the functional modules in the software were designed with encapsulation for decoupling purposes.

Proper buffering was required for both the streaming neural signals and the decoding analysis results. In online BMI experiments, although the total recording time lasted for an hour or more, only the recent recorded data contributed to the detection analysis (e.g. computation of Z-score and its confidence intervals) of the current time point. Therefore, we used a small buffer space to store the newest data and updated the buffer when new data arrived. To minimize the data

transfer cost in the buffer space, we used a circular buffering strategy; namely, the newest data always overwrote the oldest one.

The software consists of multiple task threads[44]. In order to avoid the mutual blocking between multiple tasks, we assigned different tasks on multiple threads running in parallel. The task threads included the acquisition thread, training threads, online decoding threads, user interface (UI) thread and external device controlling thread (Extended Data Fig. 2a). A custom GUI was designed and managed by the UI thread, allowing the visualization of the streaming neural signals as well as the response for user operations (Extended Data Fig. 2b).

Complete Freund's Adjuvant (CFA) administration

To induce chronic inflammatory pain, 0.1 mL of CFA (*Mycobacterium tuberculosis*, Sigma-Aldrich) was suspended in an oil saline 1:1 emulsion and injected subcutaneously into the plantar aspect of the hind paw. CFA injections were administered into the paw that was contralateral to implanted recording electrodes.

Spared nerve injury (SNI) procedure

SNI procedure was performed as described previously[45]. After rats were anesthetized with isoflurane (1.5 to 2%), the skin on the lateral surface of the thighs was incised. The bicep femoris was dissected to expose the sciatic nerve and its three terminal branches: sural, common peroneal, and tibial nerves. The common peroneal and tibial nerves were tied off with nonabsorbent 5-0 silk sutures at the proximal point of the trifurcation, and then cut distal to each knot to prevent reattachments. The muscle layer was then sutured closed with 4-0 absorbable

sutures and the skin was sutured closed with 3-0 silk sutures. SNI procedure was always done on the side contralateral to implanted recording electrodes.

Hargreaves Test (Plantar Test)

The Hargreaves test was performed to evaluate the rats' response to acute thermal stimulation. A mobile radiant heat-emitting device with an aperture of 10 mm (37370 plantar test, Ugo Basile) was used to produce acute thermal stimulation of the plantar surface of the hind paw. The rats were placed in a plexiglass chamber over a Hargreaves glass table and allowed to habituate. An average of at least 5 trials were performed to measure the latency to paw withdrawal for each testing condition. This latency was automatically recorded, and an average latency across the trials was computed. Paw withdrawals resulting from locomotion or weight shifting were not counted and the trials were repeated in such cases. Measurements were repeated at approximately 5-min intervals. An IR intensity of 70 was used to provide noxious stimulation, and intensity of 10 was used as control for thermal stimulation that was not noxious. IR stimuli were terminated by paw withdrawals or held continuously for 5 s.

For BMI experiments, the SSM was trained with 1-5 trials of noxious stimulus at the beginning of the experiment. Following this, an average of at least 5 trials were performed with activation of the BMI to test the efficacy of the BMI in inhibiting peripheral pain response. Measurements were repeated at 3-5 min intervals.

Mechanical pain detection

Rats with optic fiber and silicon probe implants were given 30 min to habituate in a plexiglass chamber over a mesh table. The SSM was trained using a noxious stimulus (pin prick, or PP, in

naive rats, and 6g von Frey filaments, or vF, in CFA- or SNI-treated rats). The noxious stimulus was applied to the plantar surface of the hind paw contralateral to the ACC recording site in free-moving rats. Noxious stimulations were terminated by paw withdrawal. Following model training, a period of rest was given the rats to avoid behavioral or neural hypersensitivity. A total of 20-25 trials were then performed with each stimulus (equal number for each stimulation type with variable inter-trial intervals) to generate Raster plots and to assess pain detection accuracy. As a control, a non-noxious stimulus (6g vF in naive rats and 0.4g vF in CFA- or SNI-treated rats) was delivered to the plantar surface of the hind paw contralateral to the brain recording site in free-moving rats. Non-noxious stimulations were applied for approximately 5 s or until paw withdrawal.

Mechanical allodynia test

A Dixon up-down method with vF filaments was used to measure mechanical allodynia[45]. Prior to testing, the rats were placed in a plexiglass container over a mesh table and acclimated for 20 minutes. A set with logarithmically incremental stiffness (0.45, 0.75, 1.20, 2.55, 4.40, 6.10, 10.50, 15.10) were applied to the hind paw in order to calculate 50% withdrawal thresholds.

For BMI experiments, CFA or SNI-treated rats with optic fiber and electrode implants were placed in a plexiglass chamber over a mesh table and allowed to habituate. 1-5 trials of 6g vF stimulus delivered to the hind paw of the rat were used to train the SSM. Subsequently the rats were allowed a period of rest to avoid hypersensitivity. The testing trials followed the Dixon up-down method. Trials with detection were used to calculate 50% withdrawal thresholds. All

stimulations were applied to the plantar surface of the hind paw contralateral to the brain recording site.

Conditioned place aversion test for evoked pain

CPA experiments were conducted in a connected two-chamber device. Animal movements in each chamber were recorded by a high-speed camera from above the chamber and analyzed with the AnyMaze software (Stoelting Co.), followed by visual verification of the recorded videos by an independent experimenter. The CPA protocol consists of preconditioning (baseline), conditioning, and testing phases. During 10-min preconditioning, the rat was allowed to move freely between the two chambers, and the time spent in each chamber was recorded. Rats that spent more than 500 s or less than 100 s in each chamber during the preconditioning phase were not used in further testing. After the training of the model, the rat was then conditioned with either BMI or random optogenetic activation of the PFC. One of the chambers was paired with BMI and the other chamber with random optogenetic activation of matching intensity, number and duration (control). The animal was confined to one of the associated chambers during each conditioning phase. During conditioning with BMI, the total number and duration of optogenetic activation events were calculated. The same number and duration of optogenetic activation was randomly delivered in the opposite control chamber. Optogenetic activation and chamber pairings were counterbalanced. The same peripheral stimulus was used in both chambers during the conditioning. PP and 6g vF (control) were used for the testing of naïve rats. For experiments with CFA- and SNI-treated rats, 6g vF and 0.4g vF (control) were used to deliver peripheral stimulus to the hind paw, whereas 6g stimulus was used to train the model. During the test phase,

388 the animal was not given any peripheral stimulus or optogenetic activation and had access to
389 move freely between the chambers. The time spent in each chamber was recorded and analyzed.
390
391 **Conditioned place aversion test for tonic pain**
392 CPA experiments were conducted for CFA- or SNI-treated rats in a connected two-chamber
393 device. Animal movements in each chamber were recorded by a high-speed camera from above
394 the chamber and analyzed with the AnyMaze software, followed by visual verification of the
395 recorded videos by an independent experimenter. The CPA protocol consists of preconditioning
396 (baseline), conditioning, and testing phases. During the 10 min of preconditioning, the rat was
397 allowed to move freely between the two chambers, and the time spent in each chamber was
398 recorded. Rats that spent more than 500 s or less than 100 s in each chamber during the
399 preconditioning phase were not used in further analysis. Following preconditioning, the SSM
400 was trained with 6g vF filament stimulation of the hind paw. During conditioning (60 min total),
401 no peripheral stimulus was given, but rats received either BMI-triggered optogenetic activation
402 of the prelimbic PFC or random PFC (control) activations of matching duration and intensity.
403 The animal was confined to one of the associated chambers during each conditioning phase.
404 During conditioning with BMI, the total number and duration of optogenetic activation events
405 were calculated, and the same number and duration of activation was randomly delivered in the
406 opposite control chamber. Furthermore, optogenetic activation and chamber pairings were
407 counterbalanced. During the test phase, the animal was not given any peripheral stimulus or
408 optogenetic activation and had access to move freely between the chambers. The time spent in
409 each chamber was recorded and analyzed.
410

Offline data statistical analysis

The neural data and behavior data were offline analyzed by custom MATLAB (Version 2018, MathWorks) scripts, NeuroExplorer (Version 5.0, NeuroExplorer) and GraphPad Prism Version 8 software (GraphPad). Online-sorted spikes were further offline spike sorted by Offline Sorter (4.0, Plexon). For each sorted neuron, a peri-stimulation time histograms (PSTH) was generated 5 s before and after the onset of the peripheral stimulus with 100 ms bin size. The normalized Z-score firing rates at each bin was calculated by the following equation: $Z = (FR - \text{mean of } FR_b) / \text{standard deviation of } FR_b$, where FR indicates firing rate and FR_b indicates baseline firing rate prior to stimulus. A positive or negative response unit was defined by at least 2 consecutive bins firing rates were higher or lower than mean of FR_b+/-3 standard deviation of FR_b within the range (0-5 s) for Hargreaves Test or (0-1 s) for PP and vF test. The cumulative firing rate was calculated by MATLAB function *trapz*. Positive pain onset detection trials were defined by SSM prediction within 5 seconds after stimulus (0-5 s). Detection rates were calculated by positive pain onset detection trials divided total stimulus trials. Student's t test was used to compare z scored firing rates across different conditions, and paired t test was used for repeated data. Fisher's exact test was used to analyze the population changes for pain response

The results of behavioral experiments were given as mean ± S.E.M. For mechanical allodynia, a one way ANOVA with repeated measures and post-hoc multiple pair-wise comparison Bonferroni tests was used to compute the 50% withdrawal threshold over time, whereas an unpaired Student's t test was used to calculate the difference in allodynia between BMI and control conditions. During the CPA test, a paired Student's t test was used to compare the time spent in each treatment chamber before and after conditioning (i.e. preconditioning vs testing

phase for each chamber). A CPA score was calculated by subtracting the time spent in the more noxious chamber during the testing phase from the time spent in that chamber during the preconditioning phase. A two-tailed unpaired Student's t test was used to compare differences in CPA scores under various testing conditions.

Immunohistochemistry

Rats were deeply anesthetized with isoflurane and transcardially perfused with ice-cold PBS. Brains were fixed in paraformaldehyde overnight and then transferred to 30% sucrose in PBS for 3 days. Next, 20μm coronal sections were collected using Leica CM3050S cryostat] (Leica Biosystems). Images containing electrodes of cannula were stained with cresyl violet and viewed using an Axio Zoom widefield microscope (Carl Zeiss).

Acknowledgments

This work was supported by NIH grants R01-NS100065 (Z.S.C., J.W.), R01-GM115384 (J.W.) and R01-MH118928 (Z.S.C.), and NSF grant CBET-1835000 (Z.S.C., J.W.).

Author contributions

J.W. and Z.S.C. conceived and designed the study; Q.Z., S.H., R.T., A.S., B.C., Z.X., D.R., A.L., and J.D.G. collected the data; Q.Z., A.S., Z.X., J.D.G., and R.T. analyzed the data; S.H., Z.X. and Z.S.C. contributed to BMI software development; J.W. and Z.S.C. supervised the project; J.W. and Z.S.C. wrote the manuscript with input from other authors.

Competing interests

The authors declare no competing interests.

1. Basbaum, A.I., Bautista, D.M., Scherrer, G. & Julius, D. Cellular and molecular mechanisms of pain. *Cell* **139**, 267-284 (2009).
2. Sadtler, P.T.*, et al.* Neural constraints on learning. *Nature* **512**, 423-426 (2014).
3. Berenyi, A., Belluscio, M., Mao, D. & Buzsaki, G. Closed-loop control of epilepsy by transcranial electrical stimulation. *Science* **337**, 735-737 (2012).
4. Bergey, G.K.*, et al.* Long-term treatment with responsive brain stimulation in adults with refractory partial seizures. *Neurology* **84**, 810-817 (2015).
5. Heck, C.N.*, et al.* Two-year seizure reduction in adults with medically intractable partial onset epilepsy treated with responsive neurostimulation: final results of the RNS System Pivotal trial. *Epilepsia* **55**, 432-441 (2014).
6. Morrell, M.J. & Group, R.N.S.S.i.E.S. Responsive cortical stimulation for the treatment of medically intractable partial epilepsy. *Neurology* **77**, 1295-1304 (2011).
7. Ajiboye, A.B.*, et al.* Restoration of reaching and grasping movements through brain-controlled muscle stimulation in a person with tetraplegia: a proof-of-concept demonstration. *Lancet* **389**, 1821-1830 (2017).
8. Taylor, D.M., Tillery, S.I. & Schwartz, A.B. Direct cortical control of 3D neuroprosthetic devices. *Science* **296**, 1829-1832 (2002).
9. Hochberg, L.R.*, et al.* Neuronal ensemble control of prosthetic devices by a human with tetraplegia. *Nature* **442**, 164-171 (2006).
10. Hochberg, L.R.*, et al.* Reach and grasp by people with tetraplegia using a neurally controlled robotic arm. *Nature* **485**, 372-375 (2012).

11. Collinger, J.L*., et al.* High-performance neuroprosthetic control by an individual with tetraplegia. *Lancet* **381**, 557-564 (2013).

12. Aflalo, T*., et al.* Neurophysiology. Decoding motor imagery from the posterior parietal cortex of a tetraplegic human. *Science* **348**, 906-910 (2015).

13. Wenger, N*., et al.* Closed-loop neuromodulation of spinal sensorimotor circuits controls refined locomotion after complete spinal cord injury. *Science translational medicine* **6**, 255ra133 (2014).

14. Wagner, F.B*., et al.* Targeted neurotechnology restores walking in humans with spinal cord injury. *Nature* **563**, 65-71 (2018).

15. Anumanchipalli, G.K., Chartier, J. & Chang, E.F. Speech synthesis from neural decoding of spoken sentences. *Nature* **568**, 493-498 (2019).

16. Turnbull, I.M. Bilateral cingulumotomy combined with thalamotomy or mesencephalic tractotomy for pain. *Surgery, gynecology & obstetrics* **134**, 958-962 (1972).

17. Rainville, P., Duncan, G.H., Price, D.D., Carrier, B. & Bushnell, M.C. Pain affect encoded in human anterior cingulate but not somatosensory cortex. *Science* **277**, 968-971 (1997).

18. Foltz, E.L. & White, L.E. The role of rostral cingulumotomy in "pain" relief. *International journal of neurology* **6**, 353-373 (1968).

19. Qu, C*., et al.* Lesion of the rostral anterior cingulate cortex eliminates the aversiveness of spontaneous neuropathic pain following partial or complete axotomy. *Pain* **152**, 1641-1648 (2011).

20. Johansen, J.P., Fields, H.L. & Manning, B.H. The affective component of pain in rodents: direct evidence for a contribution of the anterior cingulate cortex. *Proceedings of the National Academy of Sciences of the United States of America* **98**, 8077-8082 (2001).

21. LaGraize, S.C., Borzan, J., Peng, Y.B. & Fuchs, P.N. Selective regulation of pain affect following activation of the opioid anterior cingulate cortex system. *Experimental neurology* **197**, 22-30 (2006).

22. Lubar, J.F. Effect of Medial Cortical Lesions on the Avoidance Behavior of the Cat. *Journal of comparative and physiological psychology* **58**, 38-46 (1964).

23. Melzack, R.a.C., K.L. Sensory, motivational, and central control determinants of pain: a new conceptual model. . *The Skin Senses.*, 423-443 (1968).

24. Chen, Z., Zhang, Q., Tong, A.P., Manders, T.R. & Wang, J. Deciphering neuronal population codes for acute thermal pain. *Journal of neural engineering* **14**, 036023 (2017).

25. Hu, S., Zhang, Q., Wang, J. & Chen, Z. Real-time particle filtering and smoothing algorithms for detecting abrupt changes in neural ensemble spike activity. *Journal of neurophysiology* **119**, 1394-1410 (2018).

26. Lee, M*., et al.* Activation of corticostriatal circuitry relieves chronic neuropathic pain. *The Journal of neuroscience : the official journal of the Society for Neuroscience* **35**, 5247-5259 (2015).

27. Martinez, E*., et al.* Corticostriatal Regulation of Acute Pain. *Frontiers in cellular neuroscience* **11**, 146 (2017).

28. Zhang, Z*., et al.* Role of Prelimbic GABAergic Circuits in Sensory and Emotional Aspects of Neuropathic Pain. *Cell reports* **12**, 752-759 (2015).

29. Hardy, S.G. Analgesia elicited by prefrontal stimulation. *Brain research* **339**, 281-284 (1985).

30. Kiritoshi, T., Ji, G. & Neugebauer, V. Rescue of Impaired mGluR5-Driven Endocannabinoid Signaling Restores Prefrontal Cortical Output to Inhibit Pain in Arthritic Rats. *The Journal of neuroscience : the official journal of the Society for Neuroscience* **36**, 837-850 (2016).

31. Zhang, Q*., et al.* Chronic pain induces generalized enhancement of aversion. *eLife* **6**(2017).

32. Zhou, H.*, et al.* Ketamine reduces aversion in rodent pain models by suppressing hyperactivity of the anterior cingulate cortex. *Nature communications* **9**, 3751 (2018).

33. Dale, J.*, et al.* Scaling Up Cortical Control Inhibits Pain. *Cell reports* **23**, 1301-1313 (2018).

34. King, T.*, et al.* Unmasking the tonic-aversive state in neuropathic pain. *Nature neuroscience* **12**, 1364-1366 (2009).

35. Decosterd, I. & Woolf, C.J. Spared nerve injury: an animal model of persistent peripheral neuropathic pain. *Pain* **87**, 149-158 (2000).

36. De Felice, M.*, et al.* Capturing the aversive state of cephalic pain preclinically. *Annals of neurology* (2013).

37. Navratilova, E.*, et al.* Endogenous opioid activity in the anterior cingulate cortex is required for relief of pain. *The Journal of neuroscience : the official journal of the Society for Neuroscience* **35**, 7264-7271 (2015).

38. Xiao, Z.*, et al.* Cortical Pain Processing in the Rat Anterior Cingulate Cortex and Primary Somatosensory Cortex. *Frontiers in cellular neuroscience* **13**, 165 (2019).

39. Karim, F., Wang, C.C. & Gereau, R.W.t. Metabotropic glutamate receptor subtypes 1 and 5 are activators of extracellular signal-regulated kinase signaling required for inflammatory pain in mice. *The Journal of neuroscience : the official journal of the Society for Neuroscience* **21**, 3771-3779 (2001).

40. Hu, H.J., Alter, B.J., Carrasquillo, Y., Qiu, C.S. & Gereau, R.W.t. Metabotropic glutamate receptor 5 modulates nociceptive plasticity via extracellular signal-regulated kinase-Kv4.2 signaling in spinal cord dorsal horn neurons. *The Journal of neuroscience : the official journal of the Society for Neuroscience* **27**, 13181-13191 (2007).

41. O'Callaghan, J.P. & Holtzman, S.G. Quantification of the analgesic activity of narcotic antagonists by a modified hot-plate procedure. *The Journal of pharmacology and experimental therapeutics* **192**, 497-505 (1975).

42. Cheppudira, B.P. Characterization of hind paw licking and lifting to noxious radiant heat in the rat with and without chronic inflammation. *Journal of neuroscience methods* **155**, 122-125 (2006).

43. Chen, Z. *Advanced state space methods for neural and clinical data.*, (Cambridge University Press, 2015).

44. Hu S, Z.Q., Wang J, Chen Z. . A real-time rodent neural interface for deciphering acute pain signals from neuronal ensemble spike activity. *Proc. Asilomar Conf. Signals, Systems & Computers*, 93-97 (2017).

45. Wang, J*., et al.* A single subanesthetic dose of ketamine relieves depression-like behaviors induced by neuropathic pain in rats. *Anesthesiology* **115**, 812-821 (2011).

Figure Legends

Fig 1. Design of a closed-loop brain-machine interface (BMI) to detect and treat pain. a, Schematic of BMI that consists for three steps: (1) Neural recording and online signal processing including spike sorting; (2) neural decoding for pain onset detection based on sorted units; (3) pain onset detection to trigger therapeutic neurostimulation. **b,** Placement of optic fiber in the prelimbic prefrontal cortex (PFC) and recording electrodes in the anterior cingulate cortex (ACC). **c,** Left: schematic of the state-space model (SSM) for detecting the change point (pain onset) from the neuronal ensemble spike activity. Right: an example of pain onset detection using the SSM-based decoding strategy. The SSM parameters were inferred from the ACC

ensemble spike data directly in the training stage, and the Z-score (red trace) was calculated from the inferred latent variable (see **Methods**).

Fig 2. Closed-loop BMI control of acute mechanical and thermal pain. a, Schematic of BMI experiments during thermal pain delivery with an infrared (IR) emitter. Stimulus presentation lasted until paw withdrawal or 5 s. **b,** Peripheral nocifensive behavioral response to thermal stimulation. A noxious stimulus (IR 70) triggered paw withdrawals, whereas a non-noxious stimulus (IR 10) did not. n = 7-17; $p < 0.0001$, unpaired Student's t test. **c, d,** The SSM-based decoder detected the onset of a pain episode in a single trial in response to noxious stimulation (IR 70), in contrast to a trial with non-noxious stimulation (IR 10). Rasters show online sorted population spike counts with a bin size of 50 ms. The color bar indicates spike count, with the darker color representing greater spike counts. The red curve represents the estimated Z-score from the univariate latent state, and the shaded area marks the confidence intervals (see **Methods**). Horizontal dashed lines mark the thresholds for statistical significance. The vertical lines indicate the time of peripheral stimulation; red: noxious stimulus; green: non-noxious stimulus. **e,** Accuracy of SSM-based decoder in detecting acute thermal pain. n = 7-18; $p < 0.0001$, unpaired Student's t test. **f,** Schematic of SSM-decoder training and behavior testing with BMI. **g,** Pain onset detection occurred prior to withdrawal responses to noxious thermal stimulations. n = 9; $p = 0.0057$, paired Student's t test. **h,** Application of the closed-loop BMI prolonged the withdrawal latency on Hargreaves' test. No opto vs. BMI opto: n = 8; $p = 0.0074$, no opto vs. manual opto: n = 8; $p = 0.0027$, BMI opto vs. manual opto: n = 8; $p = 0.4486$, one-way ANOVA, Tukey's multiple comparisons test with repeated measures. **i,** Schematic of BMI experiments during mechanical stimulus delivery. **j,** Peripheral nocifensive behavioral response

to mechanical stimulation. A noxious stimulus (pin prick or PP) triggered paw withdrawals, whereas a non-noxious stimulus (6g von Frey filament, or vF) did not. n = 9; $p < 0.0001$, paired Student's t test. **k, l,** The SSM-based decoder detected the onset of a pain episode in a single trial in response to noxious stimulation (PP), in contrast to a trial with non-noxious stimulation (6g vF). **m,** Accuracy of SSM-based decoder in detecting mechanical pain. n = 9; $p = 0.0002$, paired Student's t test. **n,** Schematic of CPA to assess pain aversion. In a two-chamber set up, aversive response was triggered by a noxious mechanical stimulus (PP) applied to the hind paws. One of the chambers was paired with BMI, and the opposite chamber was paired with random PFC activation of matching duration and intensity. **o,** After conditioning, rats preferred BMI treatment in the presence of acute pain stimuli. n = 9; $p = 0.0007$, paired Student's t test. **p,** YFP control rats demonstrated no preference for the BMI treatment. n = 4; $p = 0.5657$, paired Student's t test. **q,** CPA scores for BMI treatment in rats that experienced acute mechanical pain. n = 4-9; $p = 0.0147$, unpaired Student's t test. **r,** Left: a representative ACC neuron increased firing rates in response to a noxious thermal stimulus (IR 70). Right: BMI reduced firing rate changes in response to the noxious stimulus. Time 0 indicates the onset of the stimulus. FR: firing rates. **s,** BMI treatment reduced the peak firing rates of pain-responsive ACC neurons in response to the noxious stimulus (see **Methods**). n = 33, $p = 0.0004$, paired Student's t test. **t**, BMI treatment reduced cumulative firing rate response of ACC neurons over a 5-s period (within the [0, 5] s range, where time 0 indicates the onset of the stimulus) in response to the noxious stimulus. n = 33, $p = 0.0135$, paired Student's t test.

Fig 3. Closed-loop BMI control of evoked pain in models of chronic inflammatory and neuropathic pain. a, Schematic for the CFA model of inflammatory pain. **b,** Peripheral

allodynia response after CFA treatment. 6g vF triggered paw withdrawals, whereas 0.4g vF did not. n = 7; p = 0.0008, paired Student's t test. **c, d,** The SSM-based decoder detected the onset of a pain episode in a single trial in response to peripheral allodynia-inducing stimulus (6g vF) in a CFA-treated rat, in contrast to a trial with a non-allodynia-inducing stimulus (0.4g vF). Population spike counts of sorted ACC units with a bin size of 50 ms. The color bar indicates spike count, with the darker color representing greater spike counts. The red curve represents the estimated Z-score from the univariate latent state, and the shaded area marks the confidence intervals. Horizontal dashed lines mark the significance thresholds. The vertical lines indicate the time of peripheral stimulation; red: noxious stimulus; green: non-noxious stimulus. **e,** Accuracy of SSM-based decoder in detecting the onset of mechanical allodynia in CFA-treated rats. n = 7; p = 0.0008, paired Student's t test. **f,** Closed-loop BMI inhibited mechanical allodynia in CFA-treated rats. n = 4-6; p = 0.0002, unpaired Student's t test. **g,** Schematic of the CPA assay in CFA-treated rats. Aversive response was triggered by an allodynia-inducing mechanical stimulus (6g vF) applied in both chambers. One of the chambers was paired with BMI, and the opposite chamber was paired with random PFC activation of matching duration and intensity. **h,** BMI treatment reduced aversion associated with mechanical allodynia (triggered by the 6g vF stimulus) in the CFA model. n = 8; p= 0.0007, paired Student's t test. **i,** YFP control rats demonstrated no preference for the BMI treatment. n = 4; p = 0.6191, paired Student's t test. **j,** CPA scores for BMI treatment in CFA-treated rats. n = 4-8; p = 0.0062, unpaired Student's t test. **k,** Schematic for the SNI model of chronic neuropathic pain. **l,** Peripheral allodynia response after SNI. 6g vF triggered paw withdrawals, whereas 0.4g vF did not. n = 6; p < 0.0001, paired Student's t test. **m, n,** The SSM-based decoder detected the onset of a pain episode in a single trial in response to peripheral allodynia-inducing stimulus (6g vF) in a SNI-treated rat, in

contrast to a trial with a non-allodynia-inducing stimulus (0.4g vF). **o,** Accuracy of SSM-based decoder in detecting mechanical allodynia in SNI-treated rats. n = 6; p = 0.0008, paired Student's t test. **p,** Closed-loop BMI inhibited mechanical allodynia in the SNI model. n = 4-5; p = 0.0004, unpaired Student's t test. **q,** Schematic of the CPA assay in SNI-treated rats. Aversive response was triggered by an allodynia-inducing mechanical stimulus (6g vF) applied in both chambers. One of the chambers was paired with BMI, and the opposite chamber was paired with random PFC activation of matching duration and intensity. **r,** BMI treatment reduced aversion associated with mechanical allodynia in the SNI model. n = 6; p = 0.0016, paired Student's t test. **s,** YFP control rats demonstrated no preference for the BMI treatment. n = 4; p = 0.4102, paired Student's t test. **t,** CPA scores for BMI treatment in SNI-treated rats. n = 4-6; p = 0.0275, unpaired Student's t test.

Fig 4. Closed-loop BMI control of spontaneous pain in chronic pain models. a, Schematic of the CPA test in the CFA model to test tonic or spontaneous pain. No peripheral stimuli were given. One of the chambers was paired with BMI, and the opposite chamber was paired with random PFC activation of matching duration and intensity. **b**, An example of sequential pain onset detection based on the SSM-based decoder in a CFA-treated rat. Arrows indicate detected onset of tonic pain episodes. **c**, CFA-treated rats prefer the BMI chamber. n = 6; p= 0.0096, paired Student's t test. **d,** YFP control rats demonstrated no preference for the BMI treatment. n = 4; p = 0.7803, paired Student's t test. **e,** CPA scores for BMI treatment in CFA-treated rats in reducing tonic pain. n = 4-6; p = 0.0140, unpaired Student's t test. **f**, Schematic of the CPA test in the SNI models to test tonic pain. No peripheral stimuli were given. One of the chambers was paired with BMI, and the opposite chamber was paired with random PFC activation. **g**, An

example of sequential pain onset detection based on the SSM-based decoder in a SNI-treated rat. Arrows indicate detected onset of tonic pain episodes. **h**, SNI-treated rats preferred the BMI chamber after conditioning. n = 6; p = 0.0127, paired Student's t test. **i,** YFP control rats demonstrated no preference for the BMI treatment. n = 4; p = 0.9456, paired Student's t test. **j,** CPA scores for BMI treatment in SNI-treated rats. n = 4-6; p = 0.0379, unpaired Student's t test.

a

③ Neurofeedback

② Neural decoding
(pain onset detection)

(trigger for
therapeutic
stimulation)

CLOSED-LOOP
BMI

Neuronal population activity

① Neural recording
& spike sorting

PFC
ACC

b

Optogenetic
stimulation

Electrode array

ACC
PrL

c

State
Space
Model
(SSM)
• • •

Observed ensemble spike counts

y_{t-1} y_t y_{t+1}

z_{t-1} z_t z_{t+1} • • •

Latent dynamic state sequences

Unit
25
20
15
10
5
-5
0
5
4
0

Inference

Z-score
5
0
-5
-5
0
5
Time (s)

a

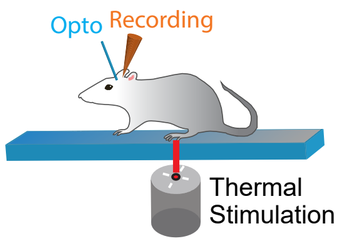

b

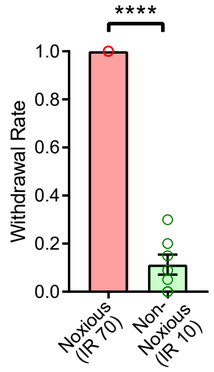

c

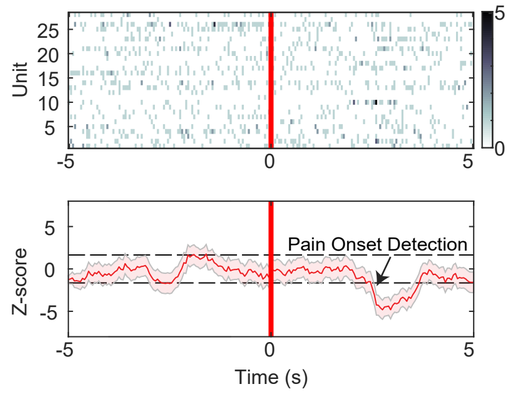

d

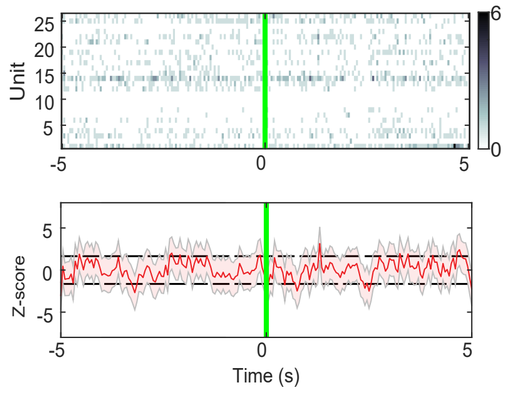

e

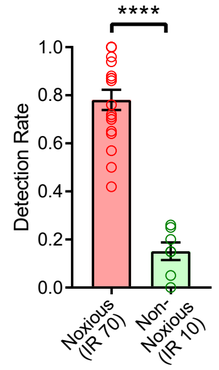

f

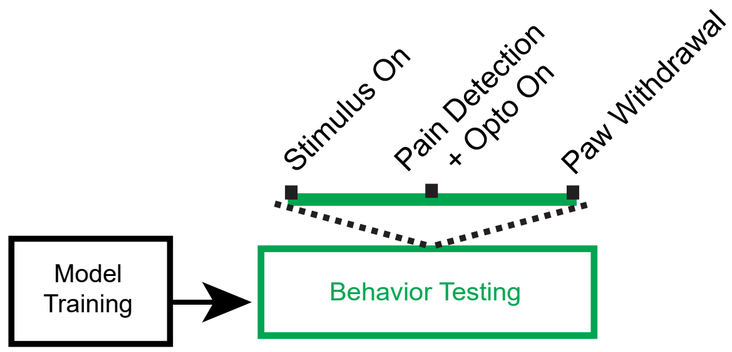

g

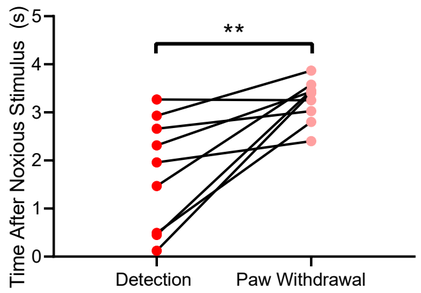

h

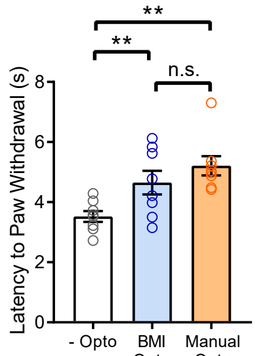

i

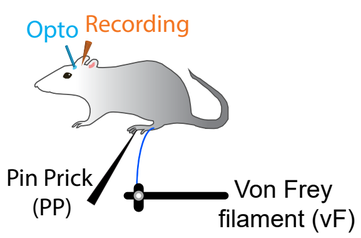

j

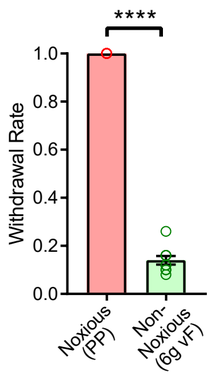

k

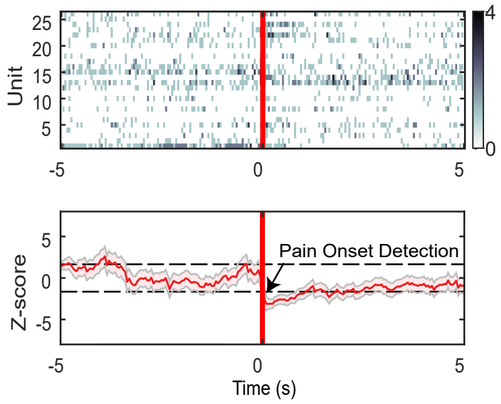

l

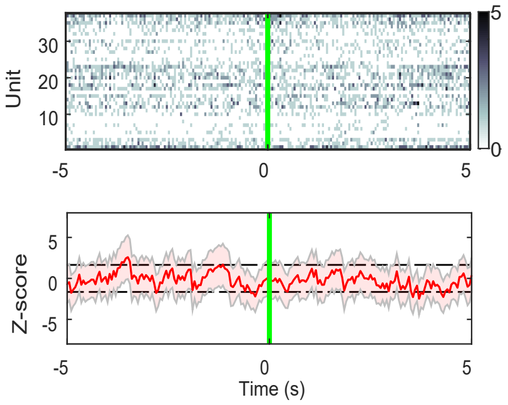

m

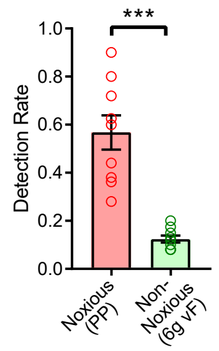

n

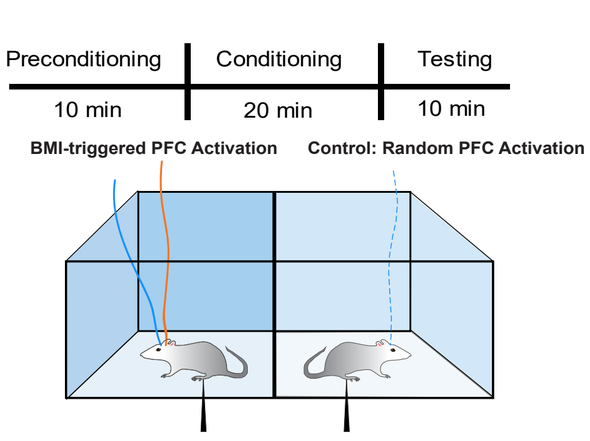

o

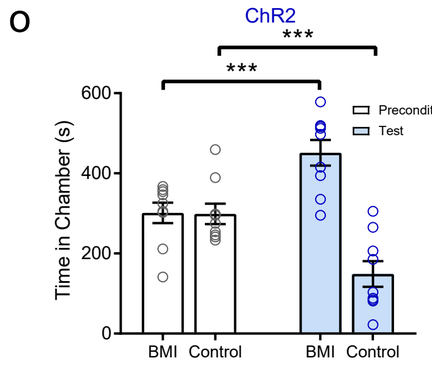

p

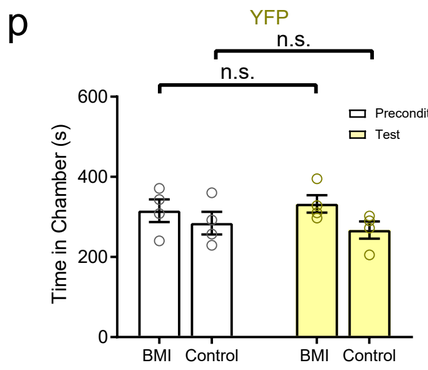

q

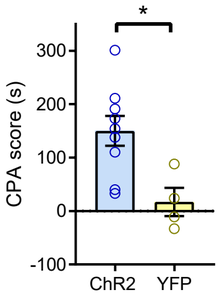

r

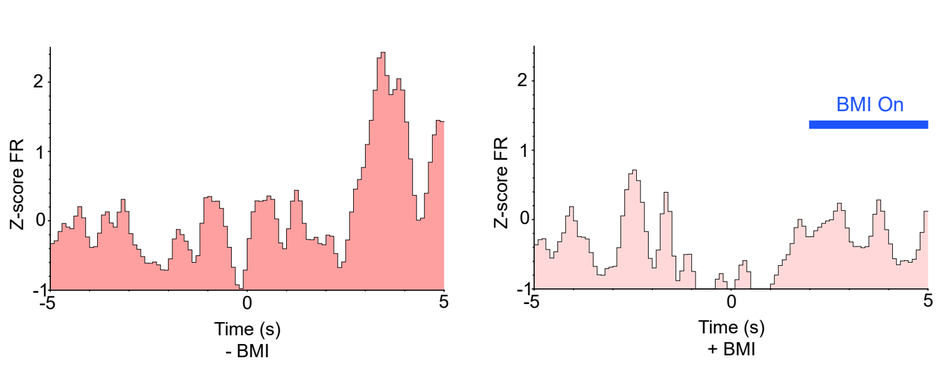

s

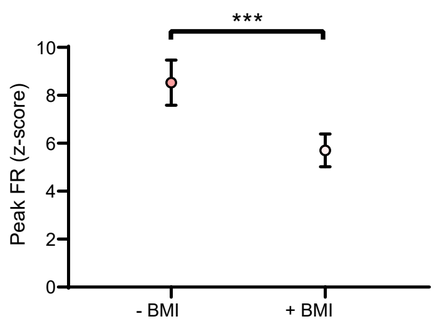

t

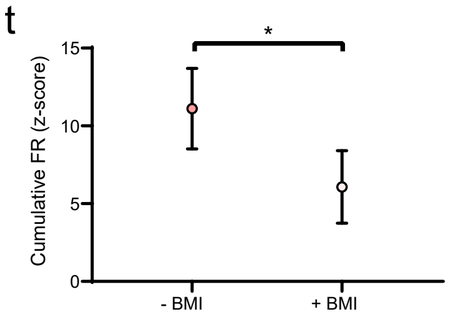

a

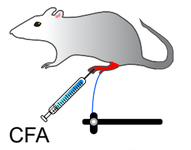

b

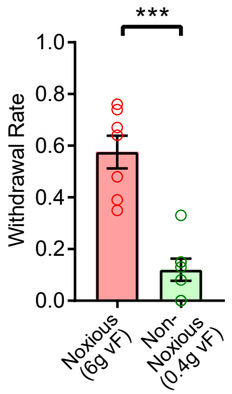

c

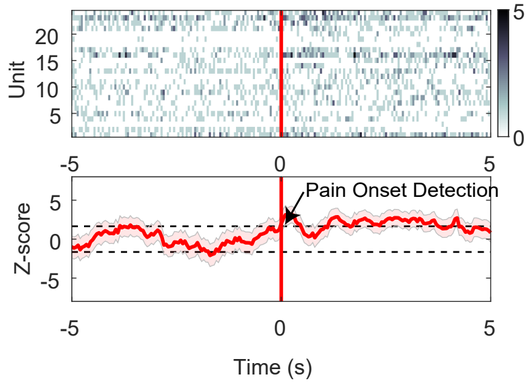

d

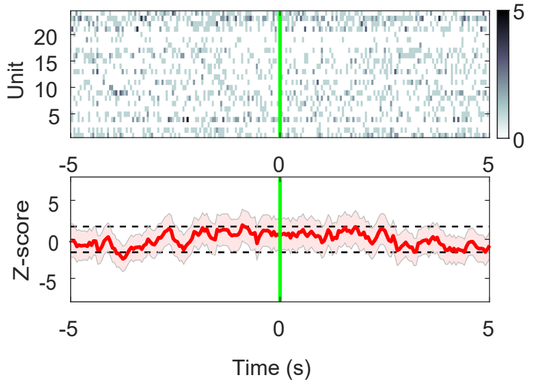

e

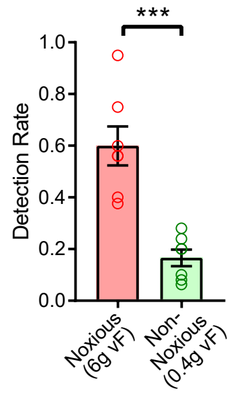

f

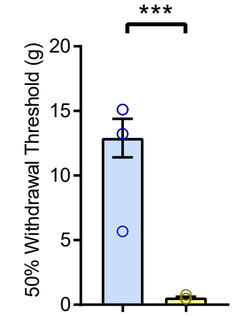

g

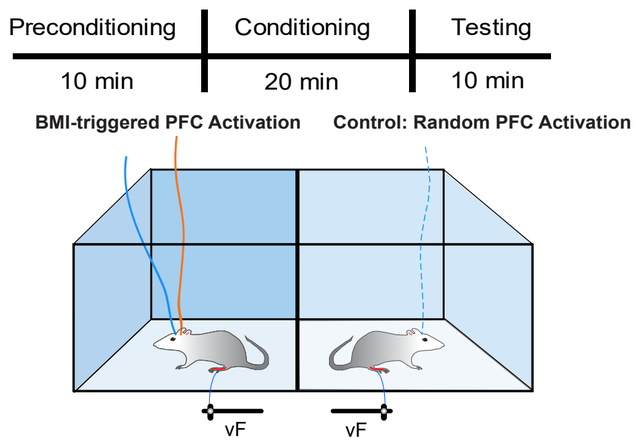

h

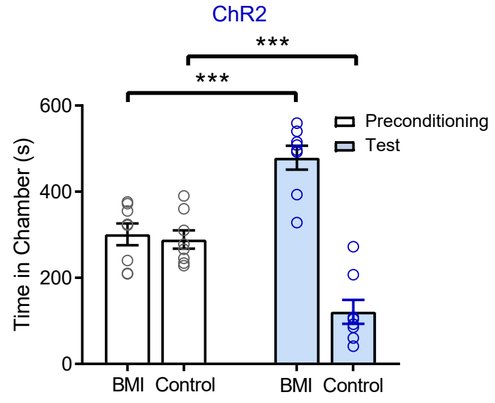

i

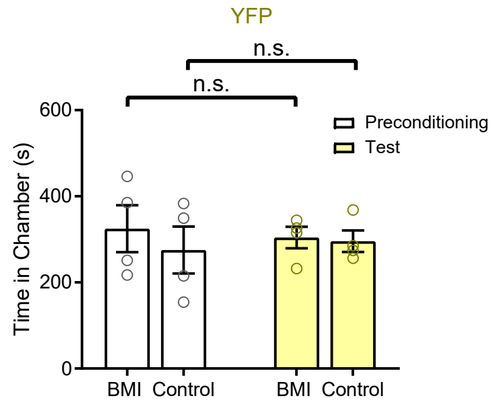

j

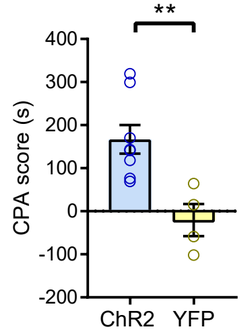

k

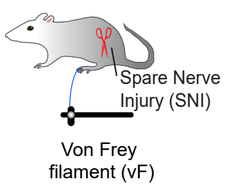

l

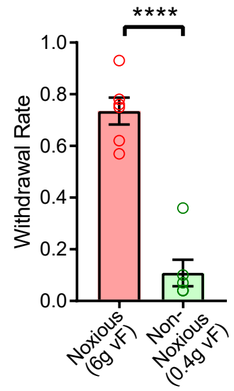

m

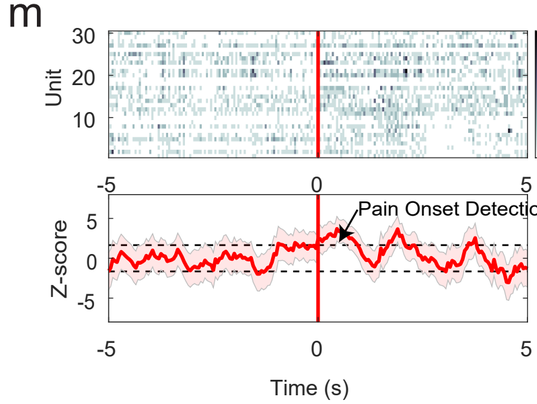

n

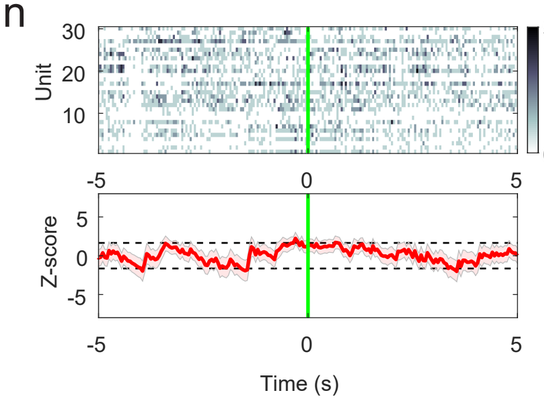

o

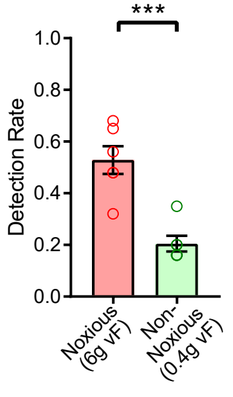

p

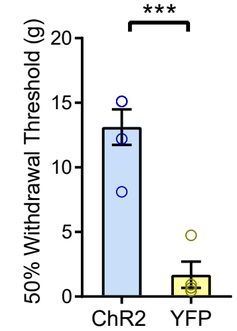

q

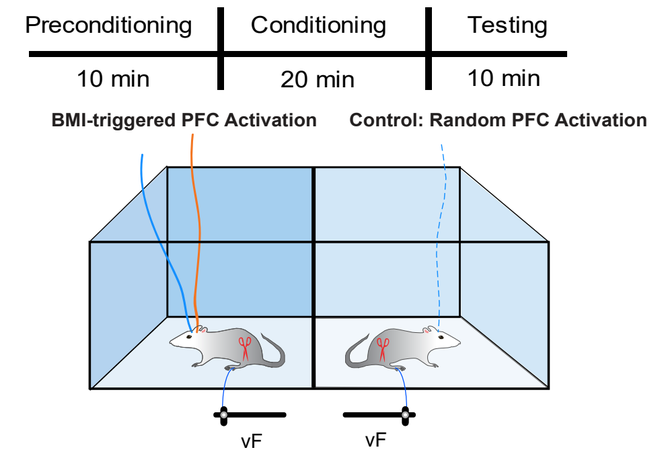

r

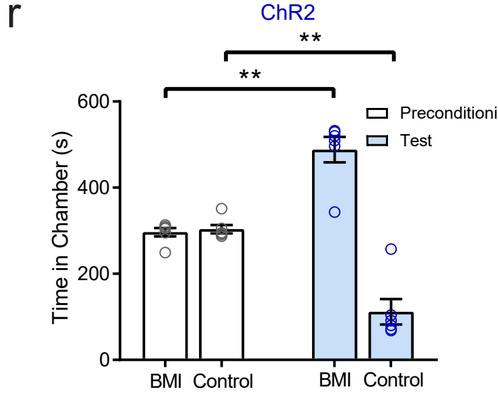

s

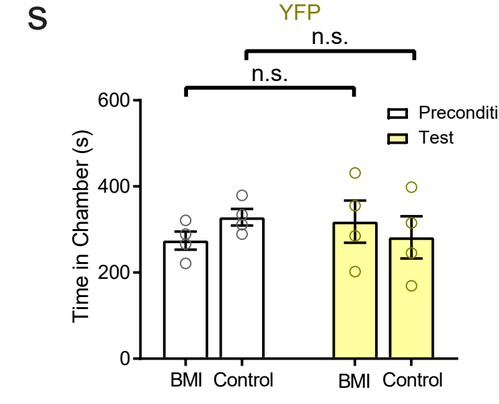

t

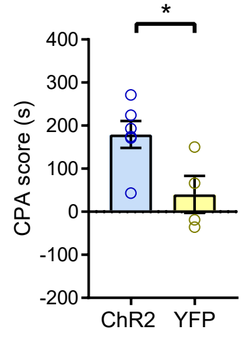

a

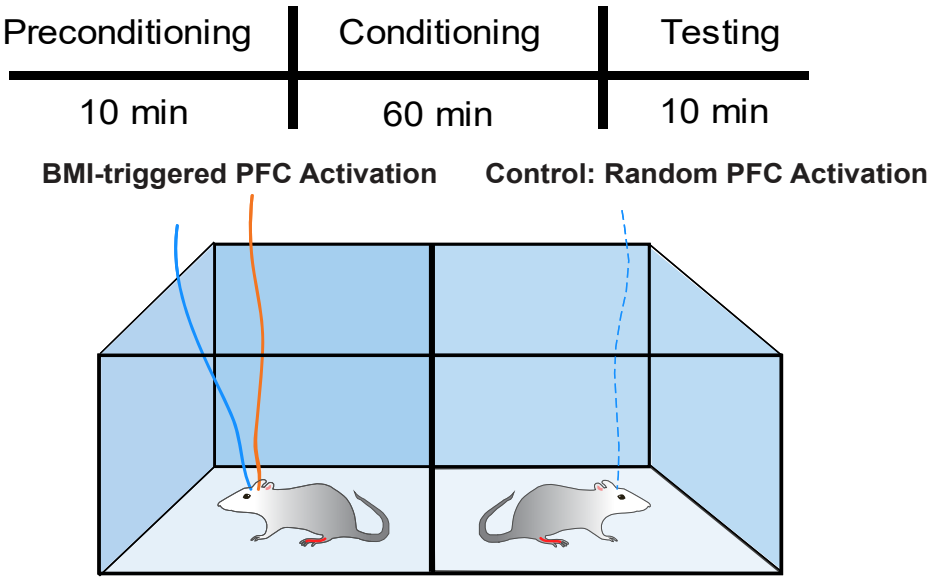
Preconditioning
Conditioning
Testing
10 min
60 min
10 min
BMI-triggered PFC Activation
Control: Random PFC Activation

b

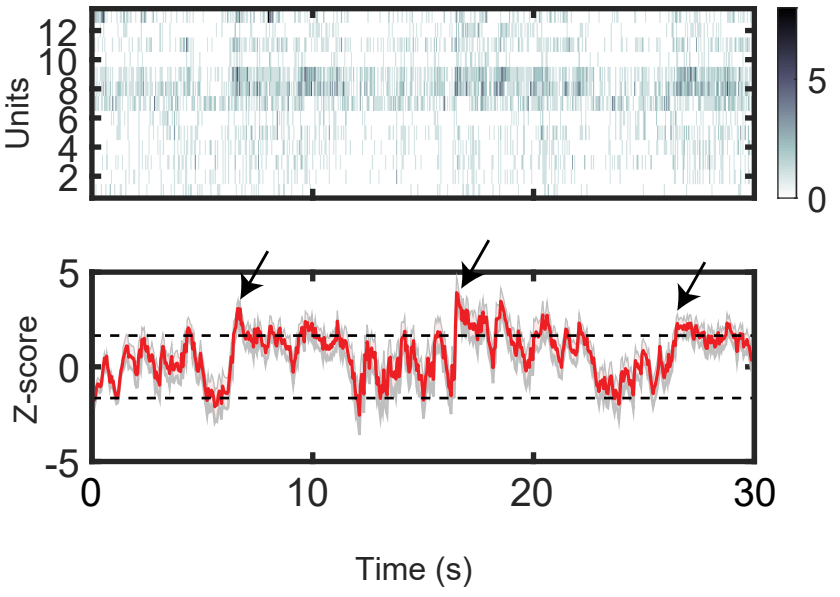
Units
12
10
8
6
4
2
5
0
Z-score
5
0
-5
0
10
20
30
Time (s)

c

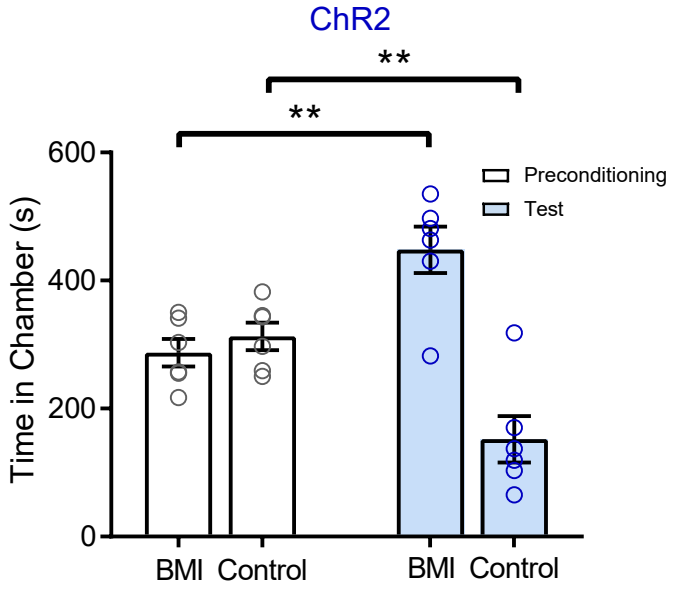
ChR2
**
**
Time in Chamber (s)
600
400
200
0
Preconditioning
Test
BMI
Control
BMI
Control

d

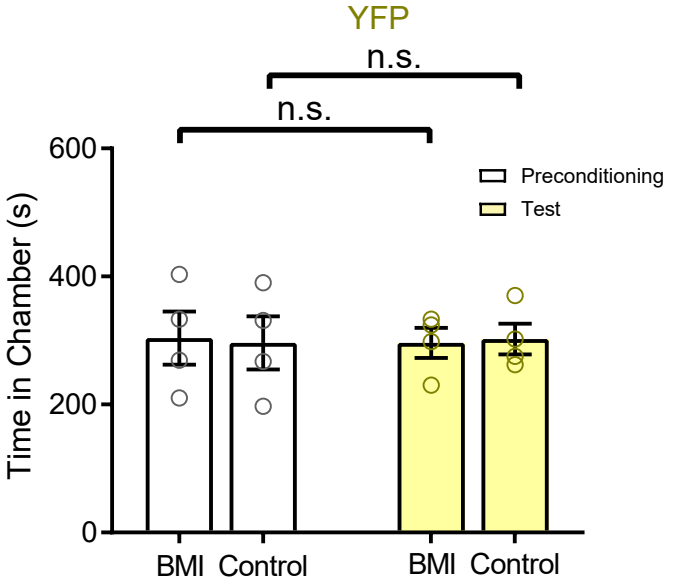
YFP
n.s.
n.s.
Time in Chamber (s)
600
400
200
0
Preconditioning
Test
BMI
Control
BMI
Control

e

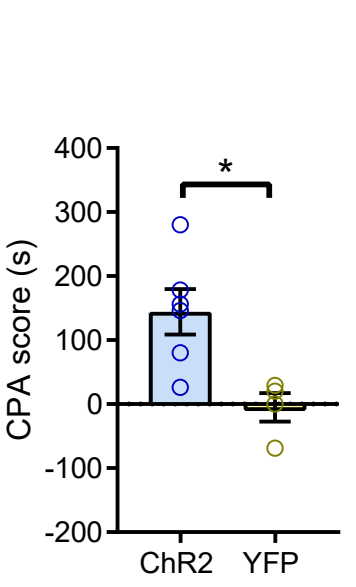
*
CPA score (s)
400
300
200
100
0
-100
-200
ChR2
YFP

f

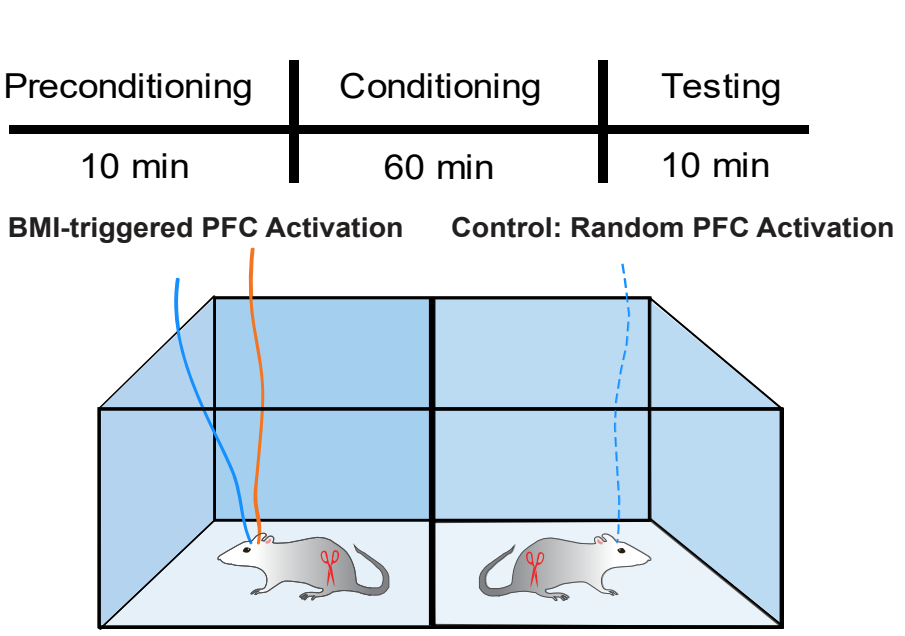
Preconditioning
Conditioning
Testing
10 min
60 min
10 min
BMI-triggered PFC Activation
Control: Random PFC Activation

g

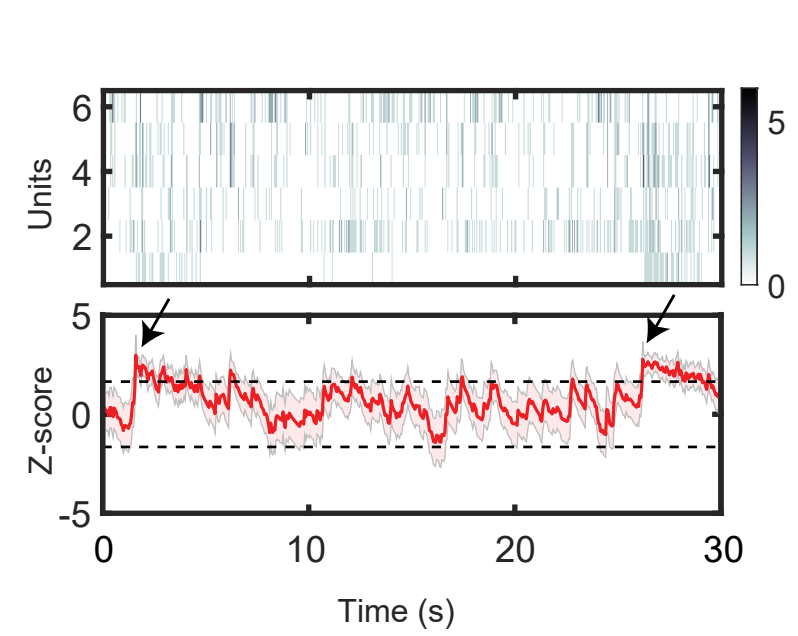
Units
6
4
2
5
0
Z-score
5
0
-5
0
10
20
30
Time (s)

h

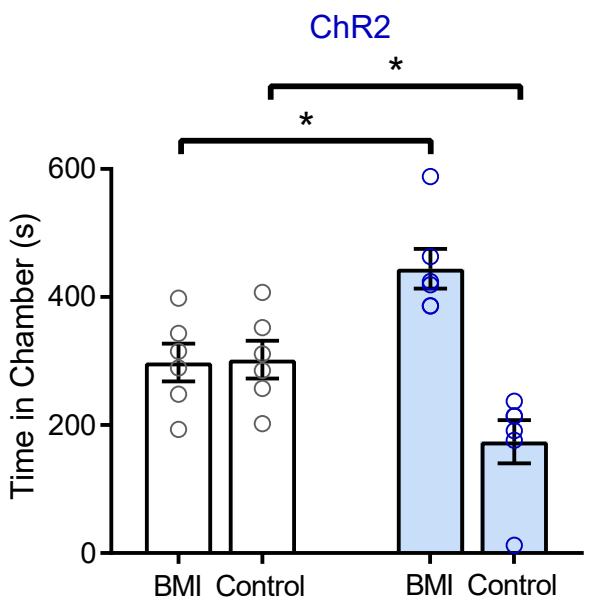
ChR2
*
*
Time in Chamber (s)
600
400
200
0
BMI
Control
BMI
Control

i

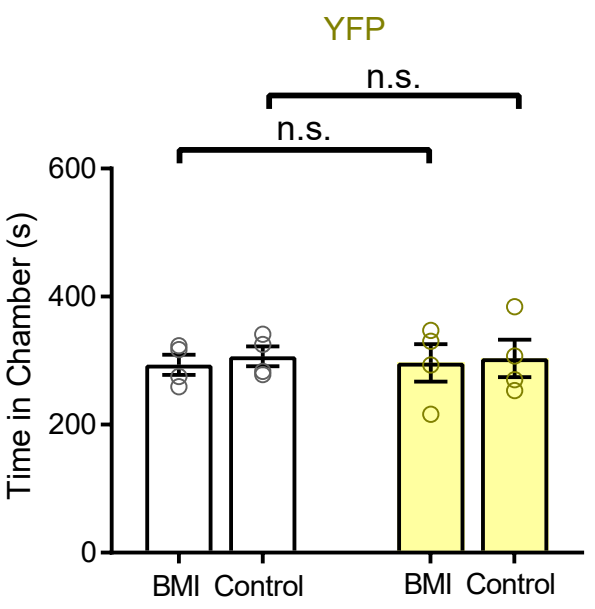
YFP
n.s.
n.s.
Time in Chamber (s)
600
400
200
0
BMI
Control
BMI
Control

j

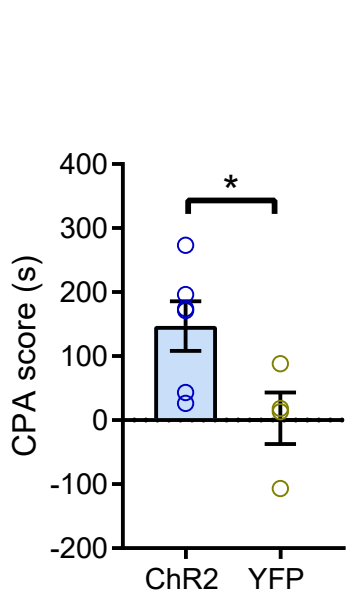
*
CPA score (s)
400
300
200
100
0
-100
-200
ChR2
YFP